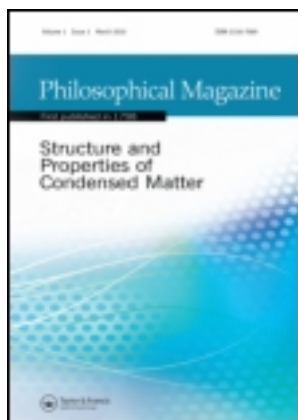


This article was downloaded by: [University of Hyderabad]

On: 09 September 2013, At: 22:40

Publisher: Taylor & Francis

Informa Ltd Registered in England and Wales Registered Number: 1072954 Registered office: Mortimer House, 37-41 Mortimer Street, London W1T 3JH, UK



Philosophical Magazine

Publication details, including instructions for authors and subscription information:

<http://www.tandfonline.com/loi/tphm20>

Structural, elastic, electronic and optical properties of layered alkaline-earth halofluoride scintillators

V. Kanchana^a, N. Yedukondalu^b & G. Vaitheeswaran^b

^a Department of Physics, Indian Institute of Technology Hyderabad, 502205, Ordnance Factory Campus Yeddumailaram, Andhra Pradesh, India

^b Advanced Centre of Research in High Energy Materials (ACRHEM), University of Hyderabad, Prof. C.R. Rao Road, Gachibowli, 500046, Hyderabad, Andhra Pradesh, India
Published online: 19 Aug 2013.

To cite this article: V. Kanchana, N. Yedukondalu & G. Vaitheeswaran (2013) Structural, elastic, electronic and optical properties of layered alkaline-earth halofluoride scintillators, *Philosophical Magazine*, 93:26, 3563-3575, DOI: [10.1080/14786435.2013.815817](https://doi.org/10.1080/14786435.2013.815817)

To link to this article: <http://dx.doi.org/10.1080/14786435.2013.815817>

PLEASE SCROLL DOWN FOR ARTICLE

Taylor & Francis makes every effort to ensure the accuracy of all the information (the "Content") contained in the publications on our platform. However, Taylor & Francis, our agents, and our licensors make no representations or warranties whatsoever as to the accuracy, completeness, or suitability for any purpose of the Content. Any opinions and views expressed in this publication are the opinions and views of the authors, and are not the views of or endorsed by Taylor & Francis. The accuracy of the Content should not be relied upon and should be independently verified with primary sources of information. Taylor and Francis shall not be liable for any losses, actions, claims, proceedings, demands, costs, expenses, damages, and other liabilities whatsoever or howsoever caused arising directly or indirectly in connection with, in relation to or arising out of the use of the Content.

This article may be used for research, teaching, and private study purposes. Any substantial or systematic reproduction, redistribution, reselling, loan, sub-licensing, systematic supply, or distribution in any form to anyone is expressly forbidden. Terms &

Conditions of access and use can be found at <http://www.tandfonline.com/page/terms-and-conditions>

Structural, elastic, electronic and optical properties of layered alkaline-earth halofluoride scintillators

V. Kanchana^a, N. Yedukondalu^b and G. Vaitheeswaran^{b*}

^aDepartment of Physics, Indian Institute of Technology Hyderabad, Ordnance Factory Campus Yeddumailaram 502205, Andhra Pradesh, India; ^bAdvanced Centre of Research in High Energy Materials (ACRHEM), University of Hyderabad, Prof. C.R. Rao Road, Gachibowli, Hyderabad 500046, Andhra Pradesh, India

(Received 21 February 2013; final version received 5 June 2013)

A systematic investigation of structural properties at ambient as well as at high pressure has been carried out for layered scintillators CaClF, CaBrF, SrClF, SrBrF and SrIF based on density functional theory. Semi-empirical dispersion correction scheme has been used to account for the van der Waals interactions and the obtained results are in good agreement with experimental data. The pressure-dependent structural and elastic properties reveal that the c-axis is more compressible than the a-axis ($C_{33} < C_{11}$) in all these materials due to weakly bonded layers stacked along the c-axis. In addition, the electronic structure and optical properties of these materials are calculated using Tran-Blaha-modified Becke-Johnson (TB-mBJ) potential. Among the five investigated compounds which are structurally anisotropic, a weak optical anisotropy is found in CaClF and SrClF and strong optical anisotropy in CaBrF, SrBrF and SrIF. The present study suggests that unlike alkaline-earth dihalides which are fast scintillators, these materials can act as storage phosphors and the possible reason is speculated from the band structure calculations.

Keywords: storage phosphor; scintillator; dispersion correction; TB-mBJ

1. Introduction

The alkaline-earth halofluorides MXF (M = Ca, Sr, Ba and X = Cl, Br, I) form an important class of materials crystallizing in the primitive tetragonal PbClF-type structure with space group $P4/nmm$ (D_{4h}^7), which is also called as the matlockite structure [1–4]. These are interesting host materials for either divalent impurities in the case of divalent alkaline-earth halofluorides (MXF) or trivalent impurities in the case of trivalent oxy halides (LaOX) at the impurity site C_{4v} [5]. SrClF : Sm⁺² has special application as a material that is more sensitive than ruby sensor which is currently used for pressure experiments in diamond-anvil cells [6,7]. SrClF_{0.5}Br_{0.5} : Sm⁺² is used for room temperature spectral hole burning [8]. BaClF : Sm⁺² can be used as a luminescence sensor in the pressure range of 5 GPa [9]. In scintillators, ionizing radiation produces electron–hole pairs, which recombine radiatively at scintillation centres to emit light. The efficiency of emitting light depends upon the transfer of energy to the scintillation site in the form of electron–hole pair. One of the key requirements for a ceramic scintillator is optical isotropy to avoid light scattering at misoriented grain

*Corresponding author. Email: gvsp@uohyd.ernet.in

boundaries [10]. Alkaline-earth dihalides such as SrI_2 [11], CaI_2 , SrBr_2 , BaX_2 ($X = \text{Cl}, \text{Br}, \text{I}$), BaIBr [10] and MSrI_3 ($M = \text{K}, \text{Rb}, \text{Cs}$) [12] are optically isotropic materials in spite of the strong anisotropy due to the non-cubic crystal symmetry. The europium-activated BaIBr [13] and SrI_2 [14] can be used for γ -ray detection due to their fast scintillating properties, whereas Eu^{+2} : CaClF , SrClF , BaClF , and BaBrF are used as X-ray storage phosphors for medical imaging via photo-stimulated luminescence [15–21] as they are less capable in transferring energy to the scintillation centre [22] when compared to the alkaline-earth dihalides. The distinct behaviour of the alkaline-earth halofluorides can be explained from their electronic structure and hence, it is very important to understand the electronic structure of these materials.

Extensive theoretical studies have been reported on alkaline-earth halofluorides using TB-LMTO method within atomic sphere approximation [23,24]. The structural and electronic properties of MXF ($M = \text{Ca}, \text{Sr}, \text{Ba}, \text{Pb}$ and $X = \text{Cl}, \text{Br}, \text{I}$) compounds were carried out by Hassan et al. [25,26] using FP-LAPW method. Using the similar method, the optical properties of MXF ($M = \text{Ba}, \text{Pb}, \text{Sr}$, and $X = \text{Cl}, \text{Br}, \text{I}$) were studied by Reshak et al. [27–29]. High pressure studies on MXF ($M = \text{Ca}, \text{Ba}, \text{Sr}$ and $X = \text{Cl}, \text{Br}, \text{I}$) compounds (with an exception of CaBrF , CaIF and SrIF) have been carried out using X-ray diffraction [30–32], in which they found a structural phase transitions to occur in BaClF and BaBrF compounds around 21 and 27 GPa, respectively. Molecular dynamics simulations were performed by Liu et al. [33] under hydrostatic pressure, in which they observed first-order phase transitions at about 28.92 and 18.04 GPa in the upstroke and downstroke processes, respectively. Using the inelastic neutron-scattering technique, the phonon frequencies of MXF ($M = \text{Ba}, \text{Sr}, \text{Pb}$ and $X = \text{Cl}, \text{Br}, \text{I}$) compounds have been measured to obtain the thermal properties such as specific heat, Debye temperature and thermal expansion coefficients [34–38]. The response of scintillating materials to the ionizing radiation can be understood from an accurate electronic structure calculation. Hence, in the present study, we have systematically investigated the structural, elastic, electronic and optical properties of CaClF , CaBrF , SrClF , SrBrF and SrIF compounds, and also studied the effect of vdW interactions on the structural properties of these layered materials at ambient conditions as well as under pressure.

The rest of the paper is organized as follows. In Section 2, we describe the computational methods used in the calculations. Results and discussion concerning the structural and elastic properties are presented in Sections 3.1 and 3.2 consists of electronic structure and optical properties and finally Section 4 concludes the paper.

2. Computational details

First-principles calculations were performed by using two distinct approaches such as planewave pseudopotential (PW-PP) and full potential linearized augmented plane wave (FP-LAPW) methods. Structural properties and their pressure dependence, elastic properties were obtained using the PW-PP approach implemented in Cambridge Series of Total Energy Package [39–41]. We have used Vanderbilt-type [42] ultra soft pseudopotentials for electron–ion interactions. Ceperly–Alder and Perdew–Zunger (CA–PZ) [43,44] parametrization of LDA and Perdew–Burke–Ernzerhof (PBE) [45] parametrization of GGA functionals were used to treat electron–electron interactions. However, the standard DFT functionals are not adequate enough to account for the nonlocal vdW interactions between layers in graphite [46] and many other layered materials [47–49] (eg. black phosphorus, see Ref. [50]). Hence, semi-empirical approaches have been developed in order to elucidate the long

range interactions in the layered materials and they were incorporated through standard DFT description. In the present study, we have used PBE+G06 scheme by Grimme [51], which is an empirical correction to DFT taking into account the dispersive interactions based on damped and atomic pairwise potentials of the form $C_6 \times R^{-6}$. Broyden-Fletcher-Goldfarb-Shanno (BFGS) minimization scheme [52] was used in geometry optimization. For each of these compounds, the following plane wave basis orbitals were used in the calculations Ca : $4s^2, 3p^6$; Sr : $5s^2, 4p^6$; F : $2s^2, 2p^5$; Cl : $3s^2, 3p^5$; Br : $4s^2, 4p^5$; I : $5s^2, 5p^5$. A proper convergence of the calculations was ensured by testing the total energy dependence on plane wave cut-off energy and k-mesh according to the Monkhorst-Pack grid scheme [53]; the cutoff energy was fixed at 450 eV and the $7 \times 7 \times 4$ k-mesh was chosen for the present calculations. The self-consistent convergence of total energy and maximum force on the atoms are found to be 5×10^{-7} eV/atom and 10^{-4} eV/Å, respectively.

The electronic structures and optical properties of these compounds were calculated using the FP-LAPW method [54] as implemented in WIEN2k package [55]. It is well known that the standard exchange-correlation functionals such as LDA [43], GGA [45], including EV-GGA [56] usually underestimate the band gap because of the simple forms that are not sufficiently flexible to accurately reproduce the exchange-correlation energy and its charge derivative. TB-mBJ [57] is a newly developed semi-local functional which uses information from kinetic energy density in addition to the charge density as employed in standard LDA or GGA functional, which can reproduce exchange energy very accurately. Hence, this semi-local functional gives improved band gaps for semiconductors and insulators. To achieve the required convergence of energy eigen values, the wave functions in the interstitial region were expanded using plane waves with a cut-off $K_{max} = 7/R_{MT}$, where R_{MT} is the smallest atomic sphere radius and K_{max} denotes the magnitude of the largest K vector in plane wave expansion. The RMT radii are assumed to be 2.25 Bohrs for Ca and Cl, 2.35 Bohrs for Sr and Br, and 2.20, 2.45 Bohrs for F and I, respectively. The wave functions inside the spheres are expanded upto $l_{max} = 10$. Self-consistency of total energy is obtained by using 45 k-points in the Irreducible Brillouin Zone (IBZ). The frequency-dependent optical properties have been calculated using 462 k-points in the IBZ.

3. Results and discussion

3.1. Crystal structure and its pressure dependence and elastic properties

The matlockite MXF (M = Ca, Sr and X = Cl, Br, I) compounds crystallize in the primitive tetragonal structure with two molecular formula units or six atoms per unit cell. The metal (Ca or Sr) and halogen (Cl, Br and I) atoms are located at $C_{4v}(4mm)$ site with atomic positions (0.25, 0.25, v), (0.75, 0.75, \bar{v}) and (0.25, 0.25, u), (0.75, 0.75, \bar{u}), respectively, whereas the fluorine atoms are at $D_{2d}(4\bar{2}m)$ symmetry site with fractional coordinates (0.75, 0.25, 0.0), and (0.25, 0.75, 0.0), where, v and u are internal variable parameters of metal (M) and halogen (X) atoms, respectively. The crystal structure is formed by layers perpendicular to the crystallographic c-axis and the sequence of layers is X-M-F-F-M-X, where F layers are doubly occupied with respect to M and X layers (see Figure 1 in Ref. [22]). In order to obtain the equilibrium structure, we have optimized both lattice geometry and ionic positions using LDA and GGA to get a fully relaxed crystal structure. The obtained equilibrium structural parameters such as lattice constants and volume are severely underestimated ($\sim 7.5-9.0\%$) with the LDA functional, while they are overestimated ($\sim 2.5-11.5\%$) using GGA functional

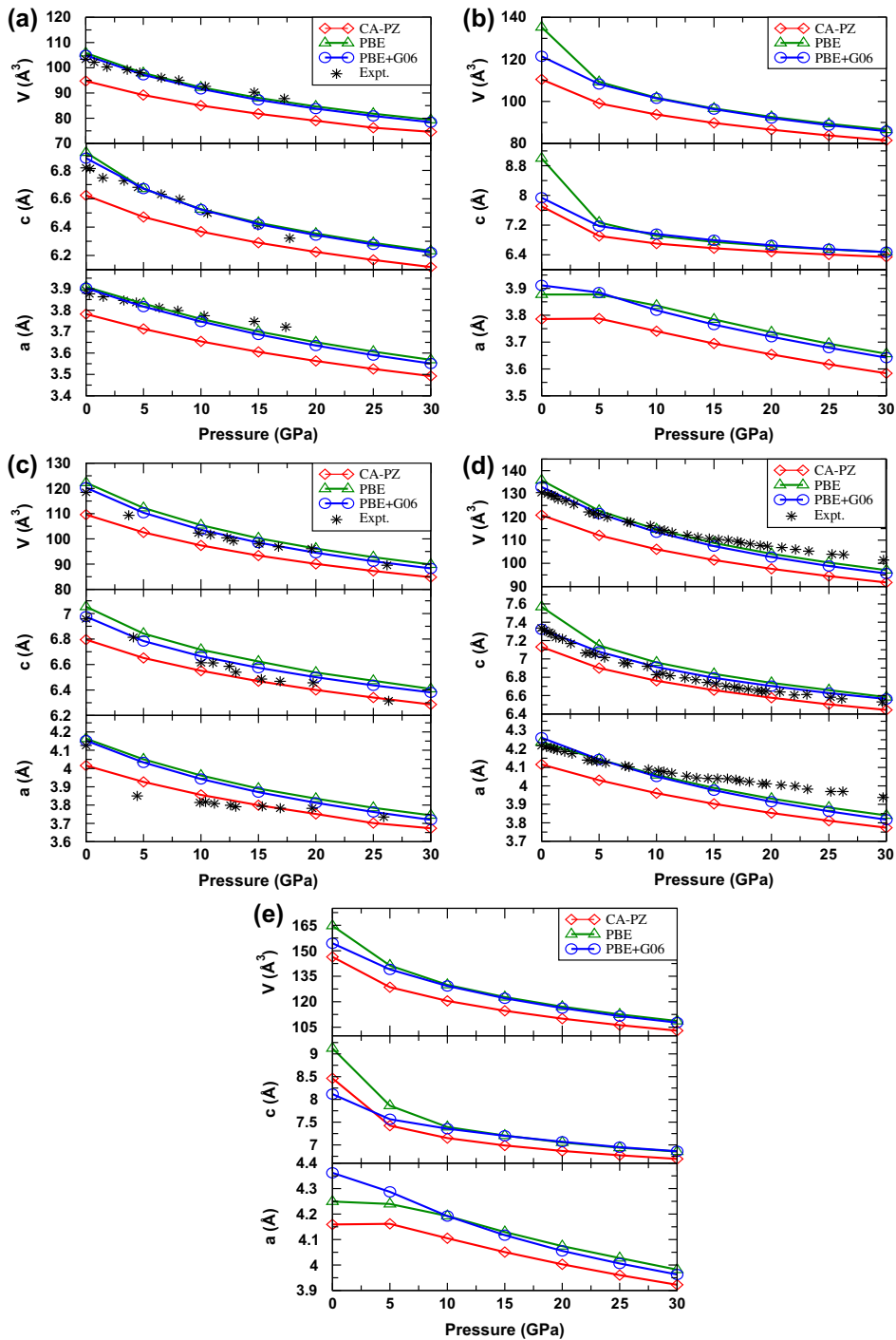


Figure 1. (colour online) Calculated lattice constants (a , c), Volume (V) of (a) CaClF, (b) CaBrF, (c) SrClF, (d) SrBrF, (e) SrIF using LDA, GGA and PBE+G06 functionals as a function of pressure. The experimental data for CaClF, SrClF and SrBrF are taken from Refs. [30,32], respectively.

Table 1. Calculated lattice constants (a, c in Å), volume (V in Å³), and fractional co-ordinates (u, v) of CaClF, CaBrF, SrClF, SrBrF and SrIF using PW-PP method are compared with experimental and other theoretical calculations.

Compound	parameter	CA-PZ	PBE	PBE+G06	Other Cal.	Expt. [2–4]
CaClF	a	3.782	3.909	3.903	3.939 ^a	3.894
	c	6.624	6.926	6.886	6.898 ^a	6.818
	V	94.76	105.85	104.92	107.03 ^a	103.38
	u	0.6422	0.6445	0.6449	0.64225 ^a	0.6432
	v	0.1970	0.1967	0.1925	0.194902 ^a	0.1962
CaBrF	a	3.786	3.877	3.911	3.926 ^a , 3.829 ^b	3.883
	c	7.707	8.999	7.938	8.139 ^a , 7.926 ^b	8.050
	V	110.47	135.30	121.44	125.45 ^a , 116.20 ^b	121.38
	u	0.6606	0.6926	0.6615	0.665408 ^a	0.670
	v	0.1676	0.1490	0.1630	0.165145 ^a	0.170
SrClF	a	4.016	4.163	4.153	4.185 ^c , 4.176 ^d , 4.163 ^e	4.126
	c	6.795	7.054	6.976	7.057 ^c , 6.99 ^d , 6.827 ^e	6.958
	V	109.60	122.26	120.29	123.60 ^c , 121.90 ^d , 118.31 ^e	118.45
	u	0.6435	0.6432	0.6442	0.6429 ^c , 0.6428 ^d , 0.664 ^e	0.6429
	v	0.2021	0.2002	0.1974	0.20152 ^c , 0.2014 ^d , 0.189 ^e	0.2015
SrBrF	a	4.116	4.237	4.261	4.084 ^b , 4.261 ^c , 4.266 ^d , 4.212 ^e	4.218
	c	7.131	7.568	7.323	7.105 ^b , 7.482 ^c , 7.436 ^d , 6.985 ^e	7.337
	V	120.81	135.87	132.95	118.50 ^b , 135.84 ^c , 135.32 ^d , 123.92 ^e	130.54
	u	0.6457	0.6992	0.6475	0.655628 ^c , 0.646 ^d , 0.668 ^e	0.6479
	v	0.1868	0.1835	0.1809	0.187089 ^c , 0.1865 ^d , 0.184 ^e	0.1859
SrIF	a	4.159	4.249	4.362	4.173 ^b , 4.305 ^c , 4.296 ^d	4.253
	c	8.463	9.123	8.116	8.667 ^b , 8.916 ^c , 8.888 ^d	8.833
	V	146.41	164.74	154.41	150.93 ^b , 165.24 ^c , 164.03 ^d	159.77
	u	0.6620	0.6627	0.6514	0.664 ^c , 0.6601 ^d	0.657
	v	0.1536	0.1517	0.1554	0.152826 ^c , 0.1545 ^d	0.167

^aRef. [25], ^bRef. [24], ^cRef. [26], ^dRef. [29], ^eRef. [37].

(in particular for CaBrF). However, the calculated structural parameters follow the expected trends of standard DFT functionals but there is large discrepancy between theoretical and experimental parameters because of the existence of vdW forces between the X-M-F-F-M-X along the c -axis. Therefore, in the present study, we have used semi-empirical dispersion correction scheme (PBE+G06) to account for the vdW forces in calculating the structural parameters of CaClF, CaBrF, SrClF, SrBrF and SrIF. The calculated equilibrium lattice parameters and volumes using PBE+G06 scheme are in excellent (~ 0.1 – 1.85%) agreement with the experimental results at ambient pressure [2–4]. Overall, we observed that vdW interactions play a major role for CaBrF and SrIF among the five investigated compounds, and a similar behaviour is also observed recently by Bjorkman et al. for these class of materials (SrIF, BaIF and PbIF) [49]. Moreover, our LDA and GGA structural parameters are also consistent with previous theoretical calculations [23–26,29,34]. All these structural parameters are summarized in Table 1 along with the experimental and theoretical data.

Table 2. Comparison between calculated elastic constants (C_{ij} in GPa) using PW-PP within PBE+G06 scheme with the available experimental and theoretical data.

Compound	Method	C_{11}	C_{33}	C_{44}	C_{66}	C_{12}	C_{13}
CaClF	Present	98.9	69.7	24.4	32.9	38.1	52.9
	Other Cal. [34]	110.8	93.2	34.8	38.2	35.7	50.5
CaBrF	Present	85.6	24.3	10.0	27.2	18.7	15.6
SrClF	Present	81.0	65.3	28.3	27.8	26.3	38.9
	Expt. [60]	93.8	76.8	28.7	31.5	29.6	–
	Expt. [61]	91.2	77.0	29.5	30.9	29.0	40.2
	Other Cal. [34]	106.1	82.9	30.6	37.9	33.2	45.8
	Other Cal. [37]	107.3	65.7	34.6	26.8	38.2	42.4
SrBrF	Present	73.6	57.7	29.4	28.9	27.6	37.6
	Expt. [36]	88.7	53.3	27.4	–	–	35.0
	Other Cal. [34]	80.9	68.2	26.1	27.9	26.1	36.9
	Other Cal. [37]	100.3	54.7	32.4	27.0	35.6	38.5
SrIF	Present	71.3	24.3	31.5	30.2	27.2	29.8
	Other Cal. [34]	65.5	55.2	20.6	22.6	21.0	30.0

High pressure studies on the structural properties of ionic-layered compounds gives a good insight on how pressure affects the weak and strong bonds in condensed matter. We have studied the structural properties of these layered materials under pressure upto 30 GPa starting from ambient pressure with a step size of 5 GPa. The PBE+G06 cell parameters are in good accordance with the available experimental data for CaClF [30], SrClF [30], and SrBrF [32] over the studied pressure range. Although the LDA (GGA) cell parameters are underestimated (overestimated) when compared to the experiment, the expected trend is well reproduced over the studied pressure range. When the PBE+G06 lattice constants (a , c) are compared at 0 and 30 GPa, the reduction in lattice constant a is 0.35Å, 0.27Å, 0.43Å, 0.44Å, and 0.40Å, while the same in lattice constant c is 0.66Å, 1.47Å, 0.59Å, 0.76Å, and 1.26Å for CaClF, CaBrF, SrClF, SrBrF, and SrIF, respectively. It is clearly observed that the reduction in the c -axis is much larger than the a -axis with increasing pressure, indicating that weakly bonded X-M-F-F-M-X layers are highly compressible, which reveals that interlayer bonding is weaker than intralayer bonding in these class of materials. It is to be noted that the GGA functional reproduced a similar trend like PBE+G06 scheme with an exception at ambient pressure, while the LDA functional follows the similar trend of underestimation over the entire pressure range studied as shown in Figure 1. Recent study on black phosphorus also shows that the standard DFT functionals are inadequate to predict the structural properties of layered materials, in particular at ambient pressure [50]. In the present work, we also show that the standard DFT functionals do not capture the vdW interactions between the layers, especially for CaBrF and SrIF compounds among the investigated compounds.

The computed PBE+G06 equilibrium volume is used to calculate elastic constants of these materials at ambient pressure. Elastic constants are fundamental parameters for crystalline solids which describe the stiffness of the solid against externally applied strains. The elastic constants were calculated using volume-conserving strains technique [58]. Due to tetragonal symmetry of the crystals, they have six independent elastic constants such

as C_{11} , C_{33} , C_{44} , C_{66} , C_{12} , C_{13} . The calculated elastic constants are positive and obey the Born's mechanical stability criteria [59], indicating that these systems are mechanically stable at ambient pressure. The elastic moduli are slightly underestimated, when compared with available experimental data (see Table 1), which might be due to the overestimation of the theoretical equilibrium volume using the PBE+G06 scheme. Overall, the obtained elastic constants are in good agreement with the available experimental results [36,60,61] as well as with shell model calculations [34,37] which are presented in Table 2. The magnitude of C_{11} is greater than C_{33} implying that these materials are stiffer along the a -axis due to strong interactions along this axis, and/or the X-M-F-F-M-X layers are weakly bonded along the c -axis, which is consistent with the fact that the lattice constant c is more compressible than a over the studied pressure range as discussed earlier. C_{66} is larger than C_{44} and C_{13} is larger than C_{12} , which again follow a similar behaviour as reported for BaXF (X = Cl, Br, I) compounds [22]. Hence, our results strongly suggest the presence of weak interlayer bonding in these layered materials consistent with pressure dependent structural properties.

3.2. Electronic structure and optical properties

The electronic structure and optical properties of CaClF, CaBrF, SrClF, SrBrF and SrIF compounds have been studied using FP-LAPW [54] method by optimizing the fractional co-ordinates at the experimental lattice parameter [2–4] within PBE-GGA. The obtained fractional co-ordinates for CaClF, $u = 0.6431$, $v = 0.1973$; for CaBrF, $u = 0.6664$, $v = 0.1648$; for SrClF, $u = 0.6429$, $v = 0.2025$; for SrBrF, $u = 0.6470$, $v = 0.1872$ and for SrIF, $u = 0.6628$, $v = 0.1544$. The calculated unit cell fractional co-ordinates are consistent with previous calculations by Hassan and Reshak et al. [25,26,29] using the same FP-LAPW method. The electronic structure of the matlockite compounds were obtained using TB-mBJ functional at ambient pressure. The calculated band structures of CaClF, CaBrF, SrClF, SrBrF and SrIF are shown in Figure 2, and their respective band gaps are 7.11, 6.14, 7.70, 6.57 and 5.28 eV with TB-mBJ functional. The electronic structures show that CaClF, SrClF, SrBrF and SrIF are direct band gap insulators with the bandgap at the Γ point, while CaBrF is an indirect band gap insulator with the separation along the $\Gamma - \Delta_{max}$ direction, which agrees quite well with the previous calculations [25]. The energy gaps obtained from PBE-GGA and EV-GGA functionals were in excellent agreement with the previous calculations [23–26,29]. From our present, previous [22] and other theoretical calculations (as mentioned above) on the mixed alkaline-earth halofluorides, it is quite evident that the TB-mBJ functional improves the bandgap significantly when compared to the other exchange correlation functionals (see Figure 3), which we have used in our calculations. Unfortunately, there are no optical spectroscopic measurements on energy gaps available for these materials to compare with our results.

In general, the electronic structure determines physical and chemical properties of materials. Europium activated BaBr [13] and SrI₂ [14] are bright and fast output scintillators while BaClF and BaBrF activated with Europium are used as X-ray storage phosphors [17–19] and the reason for this different behaviour can be explained from the band structure of these compounds [10,22]. The electronic structure of alkaline-earth halofluorides shows an important difference from alkaline-earth dihalides, which is reflected in the response of alkaline-earth halofluorides to ionizing radiation and that can be mainly due to two reasons. First, the valence band split into two distinct manifolds separated from each other as reported for BaXF (X = Cl, Br, I) compounds [22] with an exception for CaClF and SrClF, in which

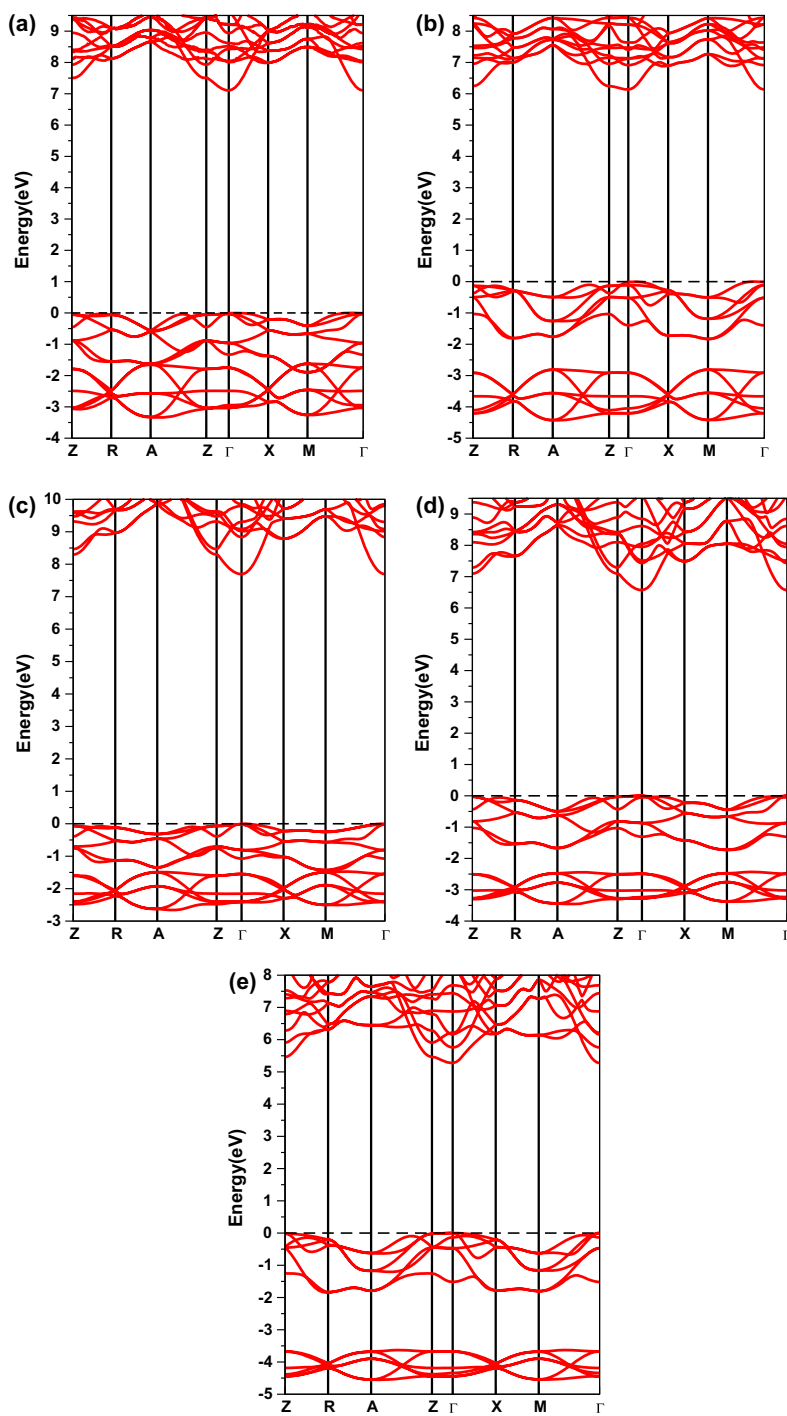


Figure 2. (colour online) Calculated band structures of (a) CaClF, (b) CaBrF, (c) SrClF, (d) SrBrF, (e) SrIF using TB-mBJ functional at the experimental lattice constants.

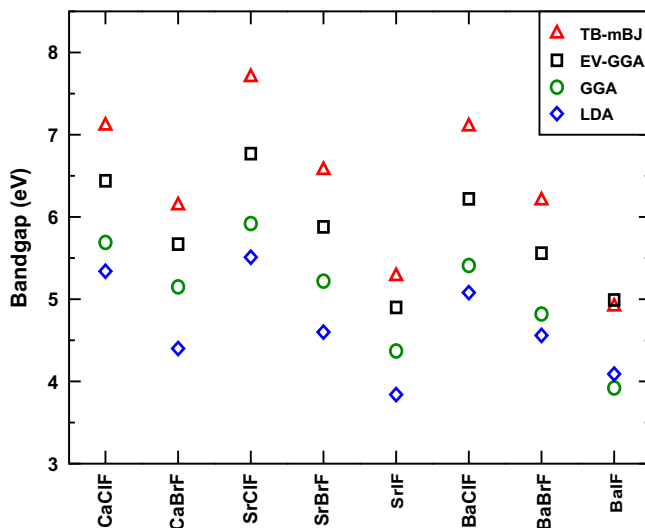


Figure 3. (colour online) Calculated LDA, GGA and EV-GGA bandgaps compared with the TB-mBJ functional for mixed alkaline-earth halofluorides. The LDA bandgaps for the compounds are taken from Refs. [25,26]; GGA, TB-mBJ, and EV-GGA band gap values for BaXF compounds are taken from Refs. [22,26].

they are almost in contact with each other because of the less electronegativity difference between F and Cl atoms. Also, the separation between the manifolds increases with atomic number because of increase in electronegativity difference between fluorine and halogens (Cl \rightarrow Br \rightarrow I) i.e. from Cl to Br, and then to I. The upper manifold is entirely derived from halogen X (Cl, Br, I) p -states, whereas, the lower manifold arises mainly from F- $2p$ states. Secondly, the ionizing radiation produces electron-hole pairs that recombine radiatively at scintillation centre in scintillators. The holes will be created on top of the halogen (X)-derived valence bands, while the electrons are in metal-derived conduction bands. Since the halogens are anions and the holes are positively charged, they would exist on X atoms between the weakly bonded X-M-F-F-M-X layers, which is a favourable situation for hole self-trapping. Hence, the radiative recombination of the electron-hole pairs (holes and electrons from X = Cl, Br, I and M = Ca, Sr ions, respectively) occurs with less probability at the scintillation site. This might be the reasons for alkaline-earth halofluorides to be used as storage phosphors rather than scintillators. A detailed discussion can be found in our previous work on BaXF compounds [22].

The energy bandgap plays a key role in determining the optical properties of materials. It is well known from the literature [10,22,57,62–64,66] that the TB-mBJ functional produces reliable energy gaps when compared to the experiments, which lead us to calculate the optical properties of CaClF, CaBrF, SrClF, SrBrF and SrIF using this TB-mBJ functional. The calculated refractive indices are shown in Figure 4. The average refractive indices at zero energy are 1.62, 1.68, 1.59, 1.68 and 1.79 and their differences between a and c -axis are 1.1%, 3.9%, 0.6%, 1.6% and 3.7% for CaClF, CaBrF, SrClF, SrBrF and SrIF respectively. The Cl-containing compounds such as SrClF and CaClF show a weak anisotropy, while the compounds containing heavier halogens such as CaBrF, SrBrF and SrIF show strong anisotropy in optical properties. It was observed from our present and

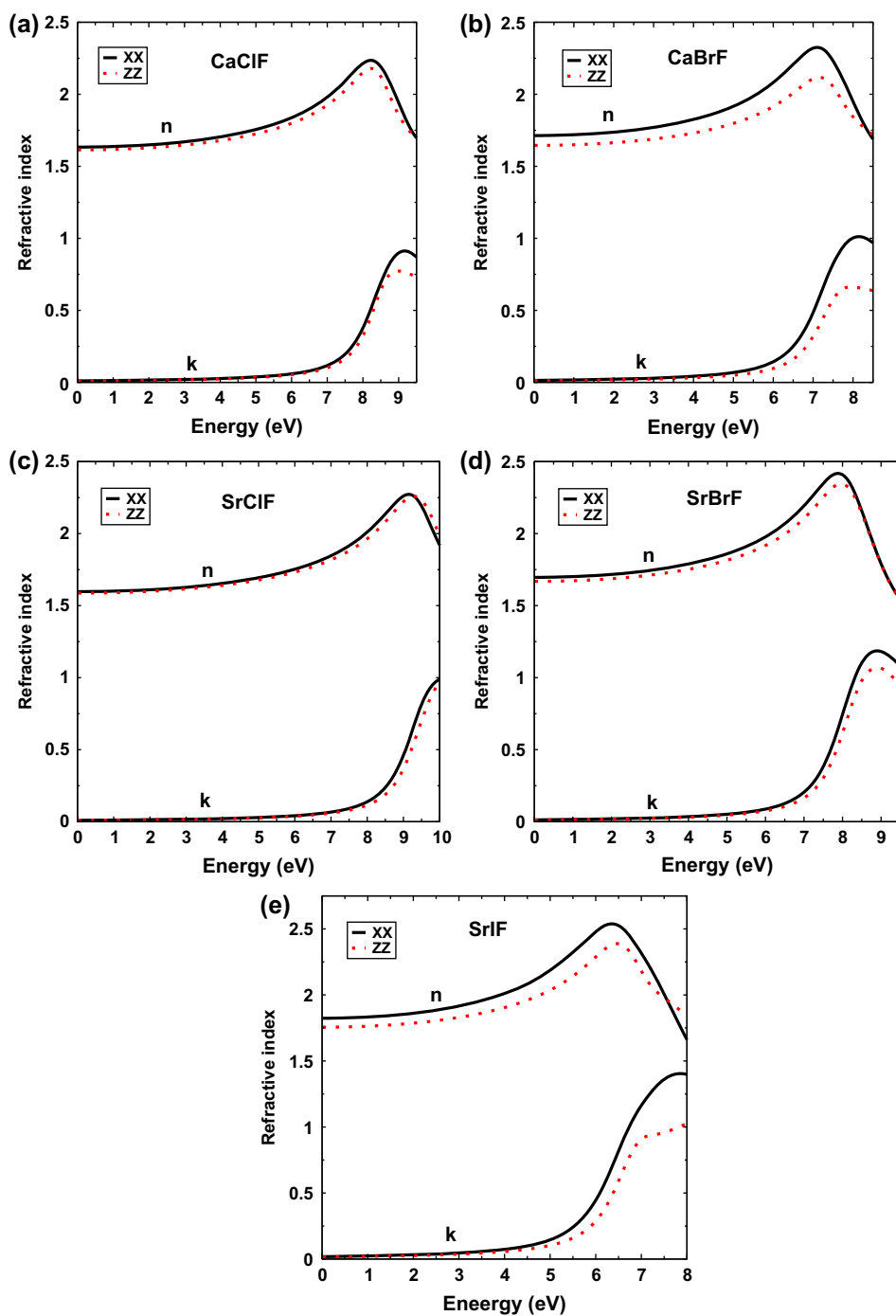


Figure 4. (colour online) Calculated optical refractive index (n) and extinction coefficient (k) of (a) CaClF, (b) CaBrF, (c) SrClF, (d) SrBrF, (e) SrIF using TB-mBJ functional at the experimental lattice constants.

previous studies [22] on PbClF-type compounds that the optical anisotropy becomes weak from Ca→Sr→Ba while it becomes stronger from Cl→Br→I. Therefore, inspite of being structurally anisotropic, we find a nearly isotropic optical properties for CaClF and SrClF. This might be favourable for the production of transparent ceramic storage phosphors based on these materials in analogy with transparent ceramic scintillators [67].

4. Conclusions

In summary, the pressure-dependent structural, and elastic properties of CaClF, CaBrF, SrClF, SrBrF and SrIF are calculated by using the PW-PP method, while the electronic structure and optical properties are studied using the FP-LAPW method. It is well known from the literature [47,48,50] that the LDA and GGA functionals are unable to predict the ground-state properties of layered materials. In the present work, we also show that the standard DFT functionals do not capture the vdW interactions between the layers in particular for CaBrF and SrIF compounds among the five investigated compounds. The calculated structural parameters using semi-empirical dispersion correction scheme (PBE+G06) are in excellent agreement with the experimental data at ambient and high pressure. The pressure dependent structural properties reveal that the *c*-axis is more compressible than *a*-axis as the X-M-F-F-M-X layers are weakly bonded along the *c*-axis and/or the interactions between the atoms along the *a*-axis are stronger. This is also confirmed by the calculated elastic constants, the elastic constant C_{33} being lesser than C_{11} in all these five compounds, implying weak interlayer bonding in these materials. The TB-mBJ functional improves the band gaps of the standard LDA and GGA functionals (see Figure 3) for all the investigated compounds. It was observed from our present and previous studies [22] on alkaline-earth halofluorides that the optical anisotropy becomes weak from Ca→Sr→Ba, while it becomes stronger from Cl→Br→I. Therefore, inspite of being structurally anisotropic, we find a nearly isotropic optical properties for CaClF and SrClF and anisotropic optical properties for CaBrF, SrBrF, and SrIF as reported for CdWO₄ scintillator [10]. Further, from the band structures of these compounds, it is clear that these compounds may act as storage phosphors in contrast to alkaline-earth dihalides which are well-known scintillators.

Acknowledgements

VK would like to acknowledge IIT-HYD for the seed grant support and NSFC awarded Research Fellowship for International Young Scientists under Grant No. 11250110051.

NYK would like to thank DRDO through ACRHEM for financial support, and the CMSD, University of Hyderabad, for providing computational facilities.

References

- [1] F. Hulliger, *Structural Chemistry of Layer Type Phases*, Dordecht:Reidel, 1975, p. 258.
- [2] B.W. Liebich and D. Nicolin, *Acta. Crystallogr. B* 33 (1977) p.2790.
- [3] H.P. Beck, *J. Solid State Chem.* 17 (1976) p.275.
- [4] M. Sauvage, *Acta. Crystallogr. B* 30 (1974) p.2786.
- [5] Y.R. Shen and W.B. Holzapfel, *Phys. Rev. B* R51 (1995) p.6127.
- [6] Y.R. Shen, T. Gregorium and W.B. Holzapfel, *High. Press. Res.* 7 (1991) p.73.
- [7] Y.R. Shen, T. Gregorium and W.B. Holzapfel, *High. Press. Res.* 12 (1994) p.91.

- [8] R. Jaaniso and H. Bill, Euro. Phys. Lett. 16 (1991) p.569.
- [9] P. Comodi and P.F. Zanazzi, J. Appl. Crystall. 26 (1993) p.843.
- [10] D.J. Singh, Phys. Rev. B 82 (2010) p.155145.
- [11] D.J. Singh, Appl. Phys. Lett. 92 (2008) p.201908.
- [12] G. Shwetha and V. Kanchana, Phys. Rev. B 86 (2012) p.115209.
- [13] E.D. Bourret-Courchesne, G. Bizarri, S.M. Hanrahan, G. Gundiah, Z. Yan and S.E. Derenzo, Nucl. Instrum. Methods Phys. Res. 613 (2010) p.95.
- [14] S.R. Podowitz, R.M. Gaume, W.T. Hong, A. Laouar and R.S. Feigelson, IEEE Trans. Nucl. Sci. 57 (2010) p.3827.
- [15] K. Rajamohan Reddy, K. Annapurna and S. Buddhudu, Mater. Lett. 28 (1996) p.489.
- [16] S. Assmann, S. Schweizer and J.-M. Spaeth, Phys. Stat. Sol. (b) 216 (1999) p.925.
- [17] R.C. Baetzold, Phys. Rev. B 36 (1987) p.9182.
- [18] K. Takahashi, K. Kohda, J. Miyahara, Y. Kanemitsu, K. Amitani and S. Shionoya, J. Lumin. 31 (1984) p.266.
- [19] K. Takahashi, J. Miyahara and Y. Shibahara, J. Electrochem. Soc. 132 (1985) p.1492.
- [20] P. Leblans, D. Vandenbroucke and P. Willems, Materials 4 (2011) p.1034.
- [21] E.D. Bourret-Courchesne, G.A. Bizarri, R. Borade, G. Gundiah, E.C. Samulon, Z. Yan and S.E. Derenzo, J. Cryst. growth 352 (2012) p.78.
- [22] N. Yedukondalu, K. Ramesh Babu, Ch Bheema lingam, D.J. Singh, G. Vaitheeswaran and V. Kanchana, Phys. Rev. B 8 (2011) p.165117.
- [23] G. Kalpana, B. Palanivel, I.B. Shameem Banu and M. Rajagopalan, Phys. Rev. B 56 (1997) p.3532.
- [24] V. Kanchana, G. Vaitheeswaran and M. Rajagopalan, J. Phys.: Condens. Matter 15 (2003) p.1677.
- [25] E.H.F. Hassan, H. Akbarzadesh and S.J. Hashemifar, J. Phys.: Condens. Matter 16 (2004) p.3329.
- [26] E.H.F. Hassan, H. Akbarzadesh, S.J. Hashemifar and A. Mokhtari, J. Phys. Chem. Solids 65 (2004) p.1871.
- [27] A.H. Reshak, Z. Charifi and H. Baaziz, Solid State Electron. 51 (2007) p.1133.
- [28] A.H. Reshak, Z. Charifi and H. Baaziz, Eur. Phys. J. B. 60 (2007) p.463.
- [29] A.H. Reshak, Z. Charifi and H. Baaziz, Physica B 403 (2008) p.711.
- [30] Y.R. Shen, V. Englisch, L. Chudinovskikh, F. Porsch, R. Haberkorn, H.P. Beck and W.B. Holzapfel, J. Phys.: Condens Matter 6 (1994) p.3197.
- [31] F. Decremps, M. Fischer, A. Polian and J.P. Itie, Phys. Rev. B 59 (1999) p.4011.
- [32] F. Decremps, M. Fischer, A. Polian and M. Sieskind, Eur. Phys. J. B. 9 (1999) p.49.
- [33] M. Liu, T. Kurobori, Y. Hirose and M. Takeuchi, Phys. Status Solidi B 225 (2001) p.R20.
- [34] M. Sieskind, A. Polian, M. Fischer and F. Decremps, J. Phys. Chem. Solids 59 (1998) p.75.
- [35] F. Decremps, M. Fischer, A. Polian and M. Sieskind, Eur. Phys. J. B. 5 (1998) p.7.
- [36] F. Decremps, M. Fischer and A. Polian, High Temp.-High Press. 30 (1998) p.235.
- [37] R. Mittal, S.L. Chaplot, A. Sen, S.N. Achary and A.K. Tyagi, Phys. Rev. B 67 (2003) p.134303.
- [38] T. Kurobori, Y. Hirose and M. Takeuchi, Phys. Status Solidi B 220 (2000) p.R11.
- [39] M.C. Payne, M.P. Teter, D.C. Allen, T.A. Arias and J.D. Joannopoulos, Rev. Mod. Phys. 64 (1992) p.1045.
- [40] V. Milman, B. Winkler, J.A. White, C.J. Packard, M.C. Payne, E.V. Akhmatkaya and R.H. Nobes, Int. J. Quant. Chem. 77 (2000) p.895.
- [41] M.D. Segall, P.L.D. Lidani, M.J. Probert, C.J. Pickard, P.J. Hasnip, S.J. Clark and M.C. Payne, J. Phys.: Condens. Matter 14 (2002) p.2717.
- [42] D. Vanderbilt, Phys. Rev. B 41 (1990) p.7892.
- [43] D.M. Ceperley and B.J. Alder, Phys. Rev. Lett. 45 (1980) p.566.
- [44] J.P. Perdew and A. Zunger, Phys. Rev. B 23 (1981) p.5048.
- [45] J.P. Perdew, S. Burke and M. Ernzerhof, Phys. Rev. Lett. 77 (1996) p.3865.

- [46] J. Harris, Phys. Rev. B 31 (1985) p.1770.
- [47] T. Björkman, A. Gulans, A.V. Krasheninnikov and R.M. Nieminen, Phys. Rev. Lett. 108 (2012) p.235502.
- [48] T. Björkman, Phys. Rev. B 86 (2012) p.165109.
- [49] T. Björkman, A. Gulans, A.V. Krasheninnikov and R.M. Nieminen, J. Phys.: Condens. Matter 24 (2012) p.424218.
- [50] S. Appalakondaiah, G. Vaitheeswaran, S. Lebégue, N.E. Christensen and A. Svane, Phys. Rev. B 8 (2012) p.035105.
- [51] S. Grimme, J. Comput. Chem. 27 (2006) p.1787.
- [52] T.H. Fischer and J. Almlof, J. Phys. Chem. 96 (1992) p.9768.
- [53] H.J. Monkhorst and J.D. Pack, Phys. Rev. B 13 (1976) p.5188.
- [54] D.J. Singh and L. Nordstrom, *Planewaves, Pseudopotentials, and the LAPW Method*, 2nd ed. Springer Verlag, Berlin, 2006,
- [55] P. Blaha, K. Schwarz, G.K.H. Madsen, D. Kvasnicka and J. Luitz, *WIEN2K, an Augmented Plane Wave + Local Orbitals Program for Calculating Crystal Properties*, Karlheinz Schwarz, Techn. UniversitatWien, Austria, 2001, ISBN: 3-9501031-1-1-2.
- [56] E. Engel and S.H. Vosko, Phys. Rev. B 47 (1993) p.13164.
- [57] F. Tran and P. Blaha, Phys. Rev. Lett. 102 (2009) p.226401.
- [58] M.J. Mehl, J.E. Osburn, D.A. Papaconstantopoulos and B.M. Klein, Phys. Rev. B 41 (1990) p.10311.
- [59] M. Born and K. Huang, *Dynamical Theory of Crystal Lattices*, Oxford University PressOxford, 1998,
- [60] M. Fischer, A. Polian and M. Sieskind, J. Phys.: Condens. Matter 6 (1994) p.10407.
- [61] K.R. Balasubramanian, T.M. Haridasan and N. Krinshamurthy, Chem. Phys. Lett. 67 (1979) p.530.
- [62] D.J. Singh, Phys. Rev. B 82 (2010) p.205102.
- [63] D. Koller, F. Tran and P. Blaha, Phys. Rev. B 85 (2012) p.155109.
- [64] D. Koller, F. Tran and P. Blaha, Phys. Rev. B 83 (2011) p.195134.
- [65] H. Dixit, R. Saniz, S. Cottenier, D. Lamoen and B. Partoens, J. Phys.: Condens. Matter 24 (2012) p.205503.
- [66] J.A. Camargo-Martínez and R. Baquero, Phys. Rev. B 86 (2012) p.195106.
- [67] A. Lempicki, C. Brecher, H. Lingertat, V.K. Sarin, US Patent No. 6 967 330, 2000.